Anthranilate Sulfonamide Hydroxamate TACE Inhibitors. Part 1: Structure-Based Design of Novel Acetylenic P1′ Groups

James M. Chen,[a,*] Guixian Jin,[a] Amy Sung[b] and Jeremy I. Levin[a,*]

[a]*Wyeth-Ayerst Research, 401N. Middletown Road, Pearl River, NY 10965, USA*
[b]*Wyeth-Ayerst Research, PO Box CN-8000, Princeton, NJ 08543, USA*

Abstract—The structure-based design of potent sulfonamide hydroxamate TACE inhibitors bearing novel acetylenic P1′ groups has led to compounds with excellent in vitro potency against TACE and selectivity over MMP-1. © 2002 Elsevier Science Ltd. All rights reserved.

Rheumatoid arthritis (RA) is a chronic debilitating autoimmune disease that results in inflammation of the joints and ultimately irreversible joint erosion.[1] It afflicts 1% of the population. The recent success of Enbrel®, a soluble tumor necrosis factor-α (TNF-α) receptor, has been a major advance in the treatment of RA patients.[2] However, the search for improved therapies with orally active agents that modulate levels of the pro-inflammatory cytokine TNF-α for RA, as well as other inflammatory diseases such as Crohn's disease, is ongoing. One avenue of exploration has been the identification of small molecule inhibitors of TNF-α converting enzyme (TACE), the enzyme responsible for the cleavage of 26 kDa membrane-bound TNF into its soluble form, a 17 kDa non-covalently bound homotrimer.[3]

This process has been aided by the fact that many of the now ubiquitous inhibitors of matrix metalloproteinases (MMPs) have also been found to inhibit TACE.[4] Examples of known TACE inhibitors include succinate hydroxamate **1**,[5] and macrocylic hydroxamic acids **2a** and **2b** (Fig. 1).[6]

In an effort to find more effective therapies for the treatment of diseases such as atherosclerosis, osteoarthritis, and cancer, as well as RA, we have recently disclosed a series of sulfonamide hydroxamic acid inhibitors of MMP-1, MMP-9, MMP-13, and TACE, based on an anthranilic acid scaffold.[7] The SAR of the anthranilic acid 3- and 5-positions (**3**, R[1] and Br) as well as the P1′ moiety (**3**, R[2]), leading to broad spectrum

MMP/TACE inhibitors exemplified by **3a** and **3b**, and the more selective TACE inhibitor **3c**, has been discussed (Fig. 2). We now wish to report on the structure-based design that has led to the discovery of novel pro-pargylic ether P1′ groups, providing potent inhibitors of TACE with selectivity over MMP-1.

The experimental structure of TACE (ADAM-17), a member of the adamalysin family of enzymes, was not known during the initial stages of our discovery effort. Since the linear sequence of TACE shares 15–28%
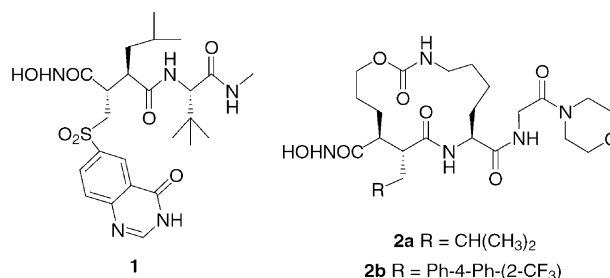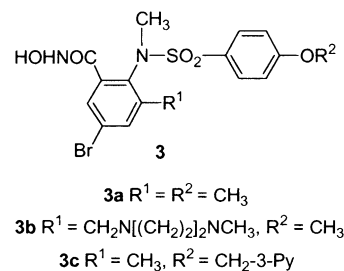

Figure 1. Literature TACE inhibitors.

2a R = CH(CH$_3$)$_2$
2b R = Ph-4-Ph-(2-CF$_3$)

Figure 2. Sulfonylated anthranilate hydroxamic acids.

3a R[1] = R[2] = CH$_3$
3b R[1] = CH$_2$N[(CH$_2$)$_2$]$_2$NCH$_3$, R[2] = CH$_3$
3c R[1] = CH$_3$, R[2] = CH$_2$-3-Py

*Corresponding authors. Tel.: +1-845-602-3053; fax: +1-845-602-5561; e-mail: levinji@war.wyeth.com (J.I.M.); tel.: +1-650-522-5269; fax: +1-650-522-5899; e-mail: jchen@gilead.com (J.M.C.)

identity with certain MMP and adamalysin sequences, and includes the consensus zinc binding motif HEXGHXLGXXH, a homology model of TACE was constructed based on its alignment with adamalysin II, with which it shares 24% identity. Construction of this model also assumed that small molecules that inhibit both MMPs and TACE would have a similar binding motif in both enzyme classes. It was hoped that this model would provide us with accurate information on the enzyme–inhibitor interaction sites, particularly in the zinc binding and S1′ regions.

Figure 3 is a partial alignment of TACE and adamalysin II showing the conserved zinc binding sequences. The three conserved histidines coordinated to the catalytic zinc metal are shown in red, as is the conserved methionine found in the Met turn. The residues in purple are the positions that define the length and depth of the S1′ pocket within the zinc metalloproteinase family. Based on the conserved nature of the amino acids in this region of the enzyme, an initial TACE homology model was constructed with a shallow S1′ pocket similar to that of MMP-1. However, this was not in accord with the potency and selectivity for TACE displayed by some of our inhibitors bearing lengthy P1′ groups.[7b] While extending the depth of the TACE S1′ pocket was unlikely, based on sequence homology, the S1′ and S3′ pockets could be connected through a channel, based on specific side-chain conformations of the leucine (blue) and valine (magenta) residues for adamalysin II in Figure 3. These correspond to the glutamate (blue) and leucine (magenta) residues of TACE in Figure 3. This channel results in an S1′ pocket that is unique in size and shape when compared to MMP-1, MMP-9, and MMP-13.

Subsequently the full catalytic domain of TACE was constructed using the COMPOSER (SYBYL) method. An iterative refinement procedure was utilized for optimizing the initial homology model.[8] The final minimized

structure of TACE had several interesting structural characteristics. First, the catalytic zinc motif was highly similar to known matrix metalloproteinases. Second, in contrast to the MMPs the model contained only the single catalytic zinc metal and no other structural metals. Finally, there were three disulfide bridges within the catalytic domain serving to stabilize the protein in the absence of structural metals.

Concurrent with this analysis, the X-ray structure of TACE with a peptide based inhibitor bound in the active site was solved at 2.0 Å.[9] Figure 4 depicts the ribbon diagrams from the TACE X-ray structure and the TACE homology model. While there are clear differences between the two structures in the outer loop regions, the areas around the active site zinc (in green) are quite similar. Figure 5 compares the S1′ binding site surface of the homology model to the X-ray structure. The three histidine residues chelating the active site zinc (red) lie to the left of the S1′ pocket. It is evident that the size and shape of the extended S1′–S3′ channel shown in the X-ray structure is highly similar to the one predicted by the homology model. Both TACE structures indicate that the S1′ pocket consists of an initial region resembling the shallow S1′ pocket of MMP-1 in size and depth. Importantly, the rest of the pocket is no longer extended linearly, as in the MMPs. Rather the extended channel is almost perpendicular to the S1′ pocket, directed toward the S3′ surface. This is clearly visible in Figure 6, in which compound **3a** is docked in the S1′ pocket described by the TACE homology model, with the zinc-chelating histidine residues on the left. As we had seen previously for analogues of **3a** bound to MMP-13, the hydroxamate of the inhibitor can chelate to the catalytic zinc in a bidentate fashion, the sulfonamide group can form a hydrogen bond with the protein backbone and the methoxyphenyl group is positioned at the entrance of the hydrophobic S1′ pocket.[10] The CH_3–O–phenyl bonds are in the eclipsed conformation pointing the methoxy group directly down the S1′–S3′ channel of TACE.

Given this information, an initial design strategy for enhancing the TACE potency and selectivity of **3a** was proposed, focusing on utilizing a carbon–carbon triple

```
ADAM II    LVAVTMAHELGHNLGMEHD......LCIMRP
TACE       EADLVTTHELGHNFGAEHD......KYVMYP
```

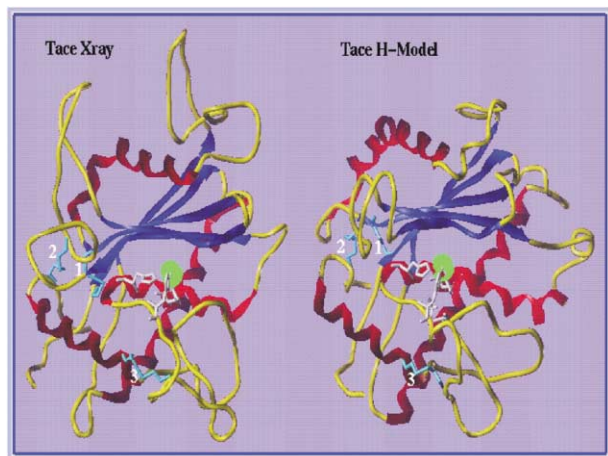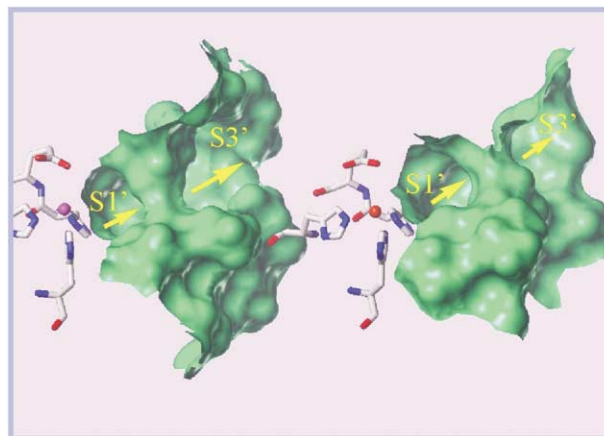**Figure 3.** Zinc binding sequences of adamalysin II and TACE.

Figure 4. Comparison of ribbon diagrams for the TACE X-ray structure (left) and TACE homology model (right).

Figure 5. Comparison of TACE active site for homology model (left) and X-ray (right), showing S1′-S3′ channel.

bond to occupy the S1′–S3′ channel (Fig. 7). Extending an acetylenic moiety from the methoxy carbon of **3a**, resulting in propargyl ether **6a**, appeared to be ideal because the shape of the acetylene matches the shape of the channel cavity, increasing favorable van der Waal's contacts with the extended channel region. It was also expected that by varying the length of the propargylic P1′ group increased selectivity for TACE could be effected. For example, the length and preferred conformation of inhibitor **6b** should provide a better fit for the S1′ pocket of TACE than for that of MMP-1, MMP-9, or MMP-13. Examination of the binding site features of the TACE model compared to the active sites of MMPs was accomplished using the analysis capabilities within SYBYL. Depicted in Figure 8 is the binding motif of designed inhibitor **6b** in the TACE homology model (gold) compared to models of MMP-1 (green) and MMP-13 (brown). In each enzyme the catalytic zinc atom (blue) is situated adjacent to the S1′ binding pocket. Among the MMPs, the structural differences between the S1′ pockets are based largely on the linear length or depth of each pocket.[11] The rigid 4-carbon chain of butynyl ether **6b**, in bent or extended conformations, cannot be accommodated in the S1′ pocket of MMP-1, MMP-9 (not shown), or MMP-13.
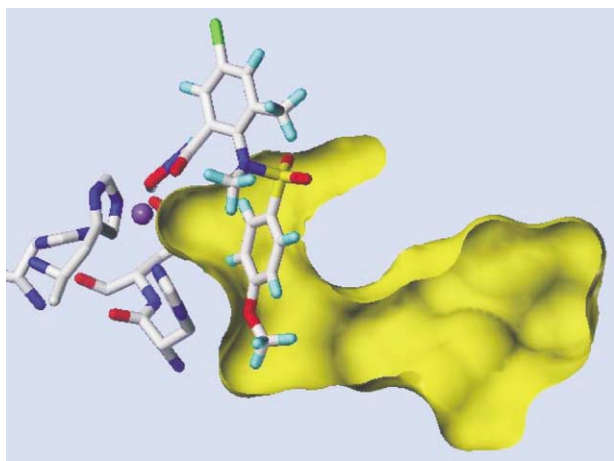
However, the shape of TACE S1′ pocket differs significantly from that of the MMPs, allowing the butynyl ether of **6b** to fit.

A series of related alkyl and propargylic ether derivatives was therefore desired to examine the effect of length and rigidity of the P1′ group on TACE potency and selectivity in vitro. The desired sulfonamide hydroxamic acids were prepared as described in Scheme 1. Thus, the desired anthranilic acid ester, **4**, was reacted with 4-fluorobenzenesulfonyl chloride and then alkylated with iodomethane to provide the 4-fluorobenzene sulfonamide, **5a**. S_NAr displacement of the fluoride of **5a** with excess 2-butyn-1-ol in the presence of sodium hydride, followed by in situ isomerization to the allenyl ether and subsequent aqueous HCl quench gave phenol **5b**.[12] Mitsunobu alkylation of phenol **5b** with the appropriate alkyl or propargylic alcohol then gave ethers **5c**. The fully functionalized anthranilate ester sulfonamides were then hydrolyzed to the carboxylic acids and converted into the hydroxamic acids, **6**, via the acid chlorides.

The in vitro activities for a series of anthranilate hydroxamates bearing alkyl and propargylic ether P1′ groups are shown in Table 1.[13] Thus, our original design target, propargyl ether **6a**, is slightly more potent against TACE than methoxy derivative **3a**, but has virtually the same TACE/MMP selectivity profile. Attaching a methyl group to the terminal acetylene of **6a** provides butynyl ether **6b**, which is essentially equipotent to **6a** against TACE enzyme. In addition, as predicted, **6b** has substantially increased selectivity for
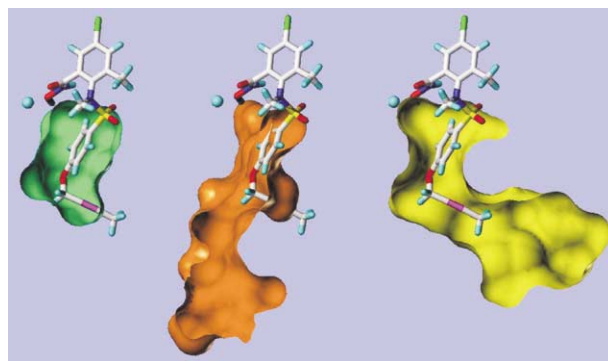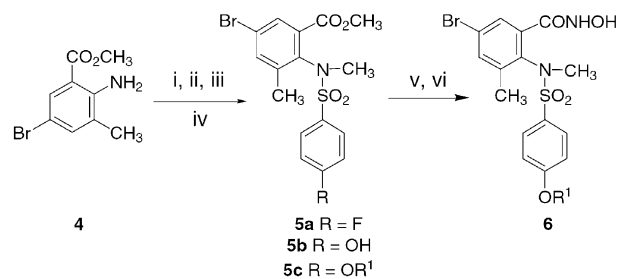
Figure 6. Inhibitor **3a** in the TACE active site with the S1′ pocket shown.
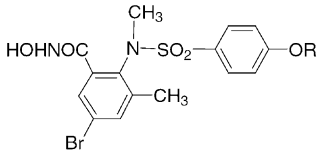
Figure 8. Designed inhibitor **6b** in the S1′ pockets of MMP-1 (left), MMP-13 (center), and TACE (right).

Scheme 1. (i) 4-F-PhSO₂Cl, TEA; (ii) CH₃I, K₂CO₃; (iii) (a) CH₃CCCH₂OH, NaH, DMF, 80 °C; (b) HCl, H₂O; (iv) R¹OH, PPh₃, DEAD; (v) NaOH; (vi) (a) (COCl)₂, DMF; (b) NH₂OH.

Figure 7. Designed propargylic ether inhibitor **6b** bound to TACE.

Table 1. In vitro activity of alkyl and propargylic ether P1′ groups

Compd	R	MMP-1[a]	MMP-9[a]	MMP-13[a]	TACE[a]
3a	CH_3	114	11	21	32
6a	CH_2CCH	113	15	52	11
6b	CH_2CCCH_3	1616	304	154	16
6c	$(CH_2)_3CH_3$	2488	21	68	67
6d	$CH_2CC(CH_2)_3CH_3$	53% (10)	389	701	34

[a]IC_{50} (nM) or % inhibition (μM).

TACE over the MMPs, validating our design strategy. In particular, **6b** is now 100-fold selective for TACE over MMP-1. That the carbon–carbon triple bond increases both TACE potency and selectivity is shown by a comparison of butynyl ether **6b** to butyl ether **6c**, which is less active against TACE and nonselective versus MMP-9 and MMP-13. Extending the acetylenic P1′ group further into the S1′–S3′ channel, as in heptynyl ether **6d**, still affords a potent inhibitor of TACE and further increases selectivity over both MMP-1 and MMP-13 relative to **6b**. Propargylic ethers **6b** and **6d** have therefore provided a dramatic improvement in TACE/MMP selectivity while retaining or improving TACE potency.

In summary, we have succeeded in utilizing structure-based computational design strategies to discover a novel series of potent TACE inhibitors with excellent selectivity over MMP-1. Acetylenic P1′ groups were suggested by a homology model of TACE that had revealed a unique S1′–S3′ channel for the enzyme, later confirmed by an X-ray crystal structure. This acetylenic P1′ moiety is also amenable to further chemical modifications, providing a handle for drug property optimization. The extension of this work to additional propargylic ether P1′ groups and their evaluation versus TACE enzyme and in a cellular assay measuring the inhibition of TNF-α production is described in the following communication.

The future therapeutic use of TACE inhibitors for the treatment of diseases modulated by TNF-α may depend on the resolution of several issues. Included among these are the determination of a desirable selectivity profile with respect to the MMPs and the ADAMs, as well as the impact of TACE inhibition on α-secretase activity. We believe that the potency and selectivity of this new class of inhibitor represents an excellent lead for the development of drugs for the treatment of rheumatoid arthritis.

References and Notes

1. Choy, E. H. S.; Panayi, G. S. *N. Engl. J. Med.* **2001**, *344*, 907.
2. Garrison, L.; McDonnell, N. D. *Ann. Rheum. Dis.* **1999**, *58* (Suppl. I), 165.
3. (a) Nelson, F. C.; Zask, A. *Exp. Opin. Invest. Drugs* **1999**, *8*, 383. (b) Lowe, C. *Exp. Opin. Ther. Pat.* **1998**, *8*, 1309. (c) Newton, R. C.; Decicco, C. P. *J. Med. Chem.* **1999**, *42*, 2295.
4. Skiles, J. W.; Gonnella, N. C.; Jeng, A. Y. *Curr. Med. Chem.* **2001**, *8*, 425.
5. Barlaam, B.; Bird, T. G.; Lambert-van der Brempt, C.; Campbell, D.; Foster, S. J.; Maciewicz, R. *J. Med. Chem.* **1999**, *42*, 4890.
6. (a) Xue, C.-B.; Voss, M. E.; Nelson, D. J.; Duan, J. J.-W.; Cherney, R. J.; Jacobson, I. C.; He, X.; Roderick, J.; Chen, L.; Corbett, R. L.; Wang, L.; Meyer, D. T.; Kennedy, K.; DeGrado, W. F.; Hardman, K. D.; Teleha, C. A.; Jaffee, B. D.; Liu, R.-Q.; Copeland, R. A.; Covington, M. B.; Christ, D. D.; Trzaskos, J. M.; Newton, R. C.; Magolda, R. L.; Wexler, R. R.; Decicco, C. P. *J. Med. Chem.* **2001**, *44*, 2636. (b) Xue, C.-B.; He, X.; Corbett, R. L.; Roderick, J.; Wasserman, Z. R.; Liu, R.-Q.; Jaffee, B. D.; Covington, M. B.; Qian, M.; Trzaskos, J. M.; Newton, R. C.; Magolda, R. L.; Wexler, R. R.; Decicco, C. P. *J. Med. Chem.* **2001**, *44*, 3351. (c) For another series of macrocyclic TACE inhibitors, see: Holms, J.; Mast, K.; Marcotte, P.; Elmore, I.; Li, J.; Pease, L.; Glaser, K.; Morgan, D.; Michaelides, M.; Davidsen, S. *Bioorg. Med. Chem. Lett.* **2001**, *11*, 2907.
7. (a) Levin, J. I.; Du, M. T.; DiJoseph, J. F.; Killar, L. M.; Sung, A.; Walter, T.; Sharr, M. A.; Roth, C. E.; Moy, F. J.; Powers, R.; Jin, G.; Cowling, R.; Skotnicki, J. S. *Bioorg. Med. Chem. Lett.* **2001**, *11*, 235. (b) Levin, J. I.; Chen, J.; Du, M.; Hogan, M.; Kincaid, S.; Nelson, F.; Venkatesan, A. M.; Wehr, T.; Zask, A.; DiJoseph, J.; Killar, L. M.; Skala, S.; Sung, A.; Sharr, M.; Roth, C.; Jin, G.; Cowling, R.; Mohler, K. M.; Black, R. A.; March, C. J.; Skotnicki, J. S. *Bioorg. Med. Chem. Lett.* **2001**, *11*, 2189. (c) Levin, J. I.; Chen, J. M.; Du, M. T.; Nelson, F. C.; Wehr, T.; DiJoseph, J. F.; Killar, L. M.; Skala, S.; Sung, A.; Sharr, M. A.; Roth, C. E.; Jin, G.; Cowling, R.; Di, L.; Sherman, M.; Xu, Z. B.; March, C. J.; Mohler, K. M.; Black, R. A.; Skotnicki, J. S. *Bioorg. Med. Chem. Lett.* **2001**, *11*, 2975.
8. Chen, J. M.; Nelson, F. C.; Levin, J. I.; Mobilio, D.; Moy, F. J.; Nilakantan, R.; Zask, A.; Powers, R. J. *J. Am. Chem. Soc.* **2000**, *122*, 9648.
9. Maskos, K.; Fernandez-Catalan, C.; Huber, R.; Bourenkov, G. P.; Bartunik, H.; Ellestad, G. A.; Reddy, P.; Wolfson, M. F.; Rauch, C. T.; Castner, B. J.; Davis, R.; Clarke, H. R. G.; Petersen, M.; Fitzner, J. N.; Cerreti, D. P.; March, C. J.; Paxton, R. J.; Black, R. A.; Bode, W. *Proc. Natl. Acad. Sci. U.S.A.* **1998**, *95*, 3408.
10. (a) Moy, F. J.; Chanda, P. K.; Chen, J. M.; Cosmi, S.; Edris, W.; Levin, J. I.; Powers, R. *J. Mol. Biol.* **2000**, *302*, 671. (b) Moy, F. J.; Chanda, P. K.; Cosmi, S.; Edris, W.; Levin, J. I.; Powers, R. *J. Biomol. NMR* **2000**, *17*, 269.
11. (a) Bode, W.; Fernandez-catalan, C.; Tschesche, H.; Grams, F.; Nagase, H.; Maskos, K. *Cell. Mol. Life Sci.* **1999**, *55*, 639. (b) Lovejoy, B.; Welch, A. R.; Carr, S.; Luong, C.; Broka, C.; Hendricks, R. T.; Campbell, J. A.; Walker, K. A. M.; Martin, R.; Van Wart, H.; Browner, M. F. *Nat. Struct. Biol.* **1999**, *6*, 217.
12. Levin, J. I.; Du, M. T. *Synth. Commun.* **2002**, in press.
13. (a) Weingarten, H.; Feder, J. *Anal. Biochem.* **1985**, *147*, 437. (b) Inhibitor concentrations were run in triplicate. MMP IC_{50} determinations were calculated from a four-parameter logistic fit of the data within a single experiment. (c) Jin, G.; Black, R.; Wolfson, M.; Rauch, C.; Ellestad, G. A.; Cowling, R., *Anal. Biochem.* **2002**, *302*, 269.